https://doi.org/10.5194/sp-2022-8
Preprint. Discussion started: 30 September 2022

STATE OF THE PLANET Discussions

Overturning and heat transport variations in the South Atlantic in an ocean reanalysis ensemble

Jonathan Andrew Baker[1], Richard Renshaw[1], Laura Claire Jackson[1], Clotilde Dubois[2], Doroteaciro Iovino[3], Hao Zuo[4], Renellys C. Perez[5], Shenfu Dong[5], Marion Kersalé[6], Michael Mayer[7,4], Johannes Mayer[7], Sabrina Speich[8], Tarron Lamont[9,10,11]

1: Met Office, UK; 2: Mercator Ocean International, France; 3: Centro Euro-Mediterraneo sui Cambiamenti Climatici, Italy; 4: European Centre for Medium-Range Weather Forecasts, UK; 5: National Oceanic and Atmospheric Administration/Atlantic Oceanographic and Meteorological Laboratory, USA; 6: Direction Générale de l'Armement, Ingénierie des projets, Paris, France 7: University of Vienna, Austria; 8: Laboratoire de Météorologie Dynamique–IPSL, Ecole Normale Supérieure, France; 9: University of Cape Town, South Africa, 10: Department of Environment, Forestry and Fisheries, Oceans and Coasts Research Branch, South Africa, 11: Bayworld Centre for Research and Education, South Africa

Correspondence to: Jonathan Baker (jonathan.baker@metoffice.gov.uk)

https://doi.org/10.5194/sp-2022-8
Preprint. Discussion started: 30 September 2022

Abstract. The variability of the South Atlantic meridional overturning circulation and meridional heat transport measured across 34.5°S during 2013–2017 differs significantly between observational and ocean reanalysis estimates. Variability in an ocean reanalysis ensemble and an eddy-resolving reanalysis is similar to an altimeter-based estimate, but smaller than energy-budget and mooring-based estimates. Over 1993-2020, there is no long-term trend in the ensemble-mean overturning and heat transport, although there are inter-model differences, whereas the altimeter-based and energy-budget estimate transports increase over this period. Time-mean overturning volume transport (and the depth of maximum overturning) across 34.5°S in the ensemble and observations are similar, whereas the corresponding mean heat transports differ by up to 0.3 PW. The seasonal cycle of these transports varies between estimates, due to differences in the methods for estimating the geostrophic flow and the sampling characteristics of the observational approaches. Thus, the mean and variation of real world South Atlantic transports, and the amplitude of their fluctuations, are still uncertain. Ocean reanalyses may be useful tools to understand these differences and the mechanisms that control volume and heat transport variability in the South Atlantic, a region critical for determining the global overturning pathways and inter-basin transports.

Short Summary. We use ocean reanalyses, in which ocean models are combined with observations, to infer past changes in ocean circulation and heat transport in the South Atlantic. Comparing these estimates with other observation-based estimates, we find differences in their trends, variability, and mean heat transport, but closer agreement in their mean overturning strength. Ocean reanalyses could help us understand the cause of these differences and thus improve estimates of ocean transports in this region.

1 Introduction

The Meridional Overturning Circulation (MOC) modulates climate on seasonal to millennial timescales via its meridional transport of freshwater, heat and carbon through the global ocean (Buckley & Marshall, 2016; Rahmstorf, 2015; Weijer et al., 2019). It is therefore important to understand how the Atlantic MOC (AMOC), which dominates the upper cell of the global MOC, is changing. Changes in overturning in the South Atlantic are particularly important because they play a crucial role in determining the pathways of the global overturning circulation (Baker et al., 2020, 2021; Nadeau & Jansen, 2020; Xu et al., 2022), while freshwater transports in the South Atlantic impact the stability of the AMOC (Garzoli & Matano, 2011; Hawkins et al., 2011; Weijer et al., 2002, 2019). Transport changes here could determine the rate at which the AMOC weakens in response to increased greenhouse gas emissions (Weijer et al., 2020; Collins et al. 2019), beyond the weakening that may have already occurred over the past century (Caesar et al., 2018; Rahmstorf, 2015; Thornalley et al., 2018).

From September 2013 to July 2017, the expanded nine-site South Atlantic Meridional Overturning Circulation – Basin-wide Array (SAMBA) (Fig 1) has collected measurements from which both daily meridional transports of heat and volume across 34.5°S can be estimated (Kersalé et al., 2020, 2021). Volume transports were also estimated during 2009-2010 using the less variable two-site pilot configuration of the SAMBA array (Meinen et al., 2013, 2018). These studies have improved our understanding of the variability of the overturning circulation

https://doi.org/10.5194/sp-2022-8
Preprint. Discussion started: 30 September 2022

and meridional heat transport (MHT) in this region. The SAMBA array has improved mooring coverage, since 2019, but data from these new sites have yet to be incorporated into AMOC estimates.

Observations of both MOC and MHT are currently only available from SAMBA during 2013-2017. Hence, longer-term variations must be inferred using model- and alternative observation-based estimates (Biastoch et al., 2021; Dong et al., 2009; Garzoli et al., 2013; Goes et al., 2015; Mignac et al., 2018). This includes transport estimates derived from satellite sea level anomalies (SLA) and in-situ data (Dong et al., 2015; Majumder et al., 2016). Although Majumder et al. (2016) found large differences between ocean reanalyses and their observation-based estimate from 2000-2014, ocean reanalyses agree better with observations than free-running models (Mignac et al., 2018). Dong et al. (2021) generated MOC and MHT estimates over 1993-2021 from a synthetic method combining in situ and satellite data (updated from Dong et al., 2015) that agreed well with XBT-derived MOC and MHT estimates in the South Atlantic. The MHT estimates from Dong et al. (2021), however, differed significantly from energy-budget MHT estimates produced by Trenberth et al. (2019). All of the aforementioned transport estimates vary less than the nine-site SAMBA array estimates (Kersalé et al., 2020, 2021).

We aim to build upon these studies by comparing an ensemble of global ocean reanalyses (product ref ‘s 1, 2, 3) directly against the observation-based estimates available over the SAMBA (2013-2017) and the altimetry (1993-2020) time periods. We also compare the reanalyses with new energy-budget MHT estimates at 34.5°S, which are analogous to an estimate at 26°N in the North Atlantic of Mayer et al. (2022), that is well correlated with observed transports across the RAPID array. While SAMBA array studies have primarily focused on daily-to-seasonal variability; here we focus on monthly-to-interannual variability. All of the time series were averaged to represent monthly values prior to further analysis.

Ocean reanalyses may provide realistic three-dimensional estimates of past changes in the South Atlantic overturning and heat transport (Mignac et al., 2018), and thus could be a useful tool to infer the nature and cause of past MOC and MHT variability. An earlier version of the reanalysis ensemble used in this study provides a good representation of the subtropical and subpolar North Atlantic overturning circulation (Jackson et al., 2018; Jackson et al., 2019; Baker et al., 2022); thus, it may also accurately simulate changes in the South Atlantic.

2 Data and Methods

We use an ensemble of eddy-permitting (¼ degree horizontal resolution) global ocean reanalyses. These are GloRanV14 (an improvement of GloSea5, MacLachlan et al., (2015)), C-GLORSv7 (Storto et al., 2016), GLORYS2V4 (Lellouche et al., 2013), and ORAP6 (Zuo et al., 2021). Together, these four reanalyses form a new Copernicus Marine Environment Monitoring Service (CMEMS) reanalyses ensemble, updating product ref 1 (see Table 1). We also use an eddy-resolving ($^1/_{12}$ degree) global ocean reanalysis, GLORYS12V1 (product ref 4). Each reanalysis uses the NEMO ocean model, but the sea-ice model and data assimilation techniques differ. Each reanalysis is constrained by observations and is driven by atmospheric forcing from either ERA5 (Hersbach et al., 2020) or ERA-Interim (Dee et al., 2011) over the period 1993-2020, with GloRan extended to December 2021.

https://doi.org/10.5194/sp-2022-8
Preprint. Discussion started: 30 September 2022

They all assimilate satellite SLA, sea-ice concentrations, and in-situ temperature and salinity, and they either assimilate satellite sea surface temperature (SST) or implement SST nudging.

We compare the MOC and MHT from the ensemble with the SAMBA-based estimates of Kersalé et al. (2020; 2021), the altimeter-based estimate of Dong et al. (2021), and the energy-budget MHT estimates of Trenberth et al. (2019) and Mayer et al. (2022).

The energy-budget estimates of Mayer et al. (2022) calculate the net surface heat flux using top-of-atmosphere radiative fluxes from CERES-EBAF (Loeb et al., 2018) with a backward extension (Liu et al., 2020), and atmospheric energy budget quantities from ERA5 (see Mayer et al., 2021 for methods). These are combined with ocean heat content (OHC) tendencies from ocean reanalyses to infer the MHT. Mayer et al. (2022) use OHC tendencies from ORAP6 ("Mayer_ORAP6" in figures); here we use an additional (unpublished) ORAS5-based estimate ("Mayer_ORAS5"), using OHC tendencies from ORAS5 (Zuo et al., 2019), the same as that used in the Trenberth et al. (2019) estimate. These ocean reanalyses were used because the monthly-mean ORAS5- and ORAP6-based inferred MHT estimates at 26°N have significant correlations with observations across the RAPID array (r=0.742 and r=0.592 respectively). We take the mean of two estimates that use either the Bering Strait or the Greenland Scotland Ridge as the northern boundary of integration. We note that energy-budget estimates may accumulate errors at southern latitudes, since they are integrated southward from high, northern latitudes (Dong et al., 2021).

Ensemble-mean and spread, and the time-mean of the altimeter-based and Mayer energy-budget estimates are calculated over 1993-2020 and over 2013-2017 SAMBA observational period. We calculate monthly-mean MOC across 34.5°S in depth coordinates, using commonly applied methods (e.g., Frajka-Williams et al., 2019), integrating monthly-mean velocity from coast-to-coast and from the surface down to the seafloor with a zero-net-volume transport constraint applied. Without this constraint, the ensemble-mean has a net southward transport through the section over the observational period of 1.14 Sv (as do the individual reanalyses), and GLORYS12v1 has a net southward transport of 3.1 Sv. For the reanalysis, the MHT is calculated by integrating the product of monthly-mean model velocity and temperature (scaled by density and specific heat coefficient) from coast-to-coast and from the surface to the seafloor with a zero-net-volume constraint applied. Each observational product applies its own constraint to reference the flow. For example, the net volume transport is not constrained to zero to calculate the overturning from the SAMBA array measurements, instead Kersalé et al. (2020a) use models to reference the time-mean barotropic component of the MOC and MHT.

We calculate the overturning profiles, the monthly-to-interannual variation, and the seasonal cycles of the upper cell MOC and the total MHT in each dataset. We separate the transports into their Ekman and geostrophic components to further investigate differences between the estimates. The Ekman component in the reanalyses is calculated using the ERA5 or ERA-Interim wind stress, and for MHT, the zonal-mean SST across the section. The geostrophic component is calculated as a residual (equivalent to combining the relative and reference transport components for the SAMBA estimates).

https://doi.org/10.5194/sp-2022-8
Preprint. Discussion started: 30 September 2022

3 Results and Discussion

The ensemble of reanalyses captures the main structure of the observed overturning profile (Fig 1a). The depth and strength of the maximum overturning is similar among all estimates with a range of ~15-18 Sv (Fig 1a). The profiles diverge in the deeper ocean, with a weaker southward flow (i.e., the overturning decreases more gradually with depth) and a weaker lower overturning cell in the ensemble than observed. The reanalyses are less accurate at depth due to fewer observations to constrain the flow. The overturning profiles of the ensemble and GLORYS12V1 in density space have a stronger maximum overturning transport than that calculated in depth space, and they have no negative transport (i.e., no abyssal cell) (Fig 1b). Thus, obtaining the overturning in density space may be important to accurately infer the overturning pathways across 34.5°S. We focus herein on the MOC in depth space because the temporal variability of the upper MOC strength in the reanalyses is fairly insensitive to the coordinate system (not shown), and they can then be directly compared with the other estimates.

We now analyse the basic statistics of the variability of the maximum overturning strength and the MHT by looking at their time-mean and standard deviation over the 2013-2017 mooring observational period and over 1993-2020. The time-mean overturning estimates have a range of 15.5 – 18.7 Sv, with the ensemble-mean (labelled "mean" in figures) being only slightly weaker than the altimeter-based estimate and that observed across SAMBA (crosses in Fig 2a), and the range in mean values is within the documented uncertainty of SAMBA (Table 2). In contrast, the time-mean MHT estimates have a relatively large range of 0.35 – 0.61 PW (crosses in Fig 2c), although the ensemble-mean is within the uncertainty range of SAMBA. This increased spread in the time-mean MHT compared to the MOC (even without the energy-budget MHT estimates) could be due to variations in the inferred temperature field or spatial distribution of velocity. The ensemble-mean MHT is similar to the energy-budget estimates based on Mayer et al. (2022) (Fig 2c). While there is inter-model spread in the ensemble time-mean transports (crosses in Fig 2b,d), the spread is smaller than the uncertainty in SAMBA (Table 2), although it is more comparable for the MHT than for the MOC. We note that time-mean transports in SAMBA are calculated using time-mean reference velocities from a model (Kersalé et al., 2020). We focus herein on the variation of transport anomalies from their time-mean values.

Monthly-mean variability (i.e., the standard deviation) of overturning and MHT in the ensemble have a similar magnitude to the altimeter-based estimate over both the 2013-2017 mooring observational period and 1993-2020, whereas variability observed from SAMBA is far greater (Fig's 2a,c and 3, and Table 2), with significant ($p < 0.05$) differences (in an F-test for equality of two variances). Similarly, the ensemble-mean timeseries is significantly ($p < 0.05$) correlated with the altimeter-based estimate ($r = 0.63$ for MOC and $r = 0.77$ for MHT over the observational period), but is not well correlated with SAMBA ($r < 0.1$). The monthly-mean SAMBA estimates have large high-frequency variations (Fig 3a,b). These high-frequency variations could be caused by ocean eddy variability and barotropic variations that were previously under-resolved with only two mooring sites, and are now better resolved but likely still aliased with nine sites. The Mayer energy-budget MHT estimates also have high-frequency variations of a magnitude comparable to SAMBA (Fig 3b,d and Table 2), although their variability is uncorrelated with SAMBA. "Mayer_ORAP6" is weakly but significantly ($p < 0.05$) correlated with the ensemble-mean ($r = 0.14$) and altimeter-based estimate ($r=0.19$) over 1993-2017, and with the altimeter-based estimate ($r = 0.32$) over the SAMBA period. "Mayer_ORAS5" has a higher correlation with the ensemble ($r =$

https://doi.org/10.5194/sp-2022-8
Preprint. Discussion started: 30 September 2022

0.30) and altimeter-based estimate (r = 0.32) over 1993-2017, and with the ensemble (r = 0.52) and altimeter-based estimate (r = 0.57) over the SAMBA period. The GloRan reanalysis run without assimilating altimetry data (not shown) is still significantly correlated with the altimeter-based estimate (r = 0.54). Thus, the strong correlation between ensemble and altimeter-based estimates is not due to both using altimetry data. We note, however, that the experimental reanalysis still assimilates in situ and satellite temperature and salinity data, some of which is used in the altimeter-based estimate, so the ensemble and altimeter-based estimate are not completely independent.

The GLORYS12V1 reanalysis has a stronger time-mean MOC and MHT than the ensemble-mean (and GLORYS2V4). It has similar monthly-mean variability to the ensemble, slightly larger than the ensemble-mean, but smaller than GLORYS2V4 (Table 2). GLORYS12V1 is also significantly correlated with the ensemble-mean (r = 0.80 for MOC; r = 0.84 for MHT, over 1993-2019). Thus, fully resolving (as opposed to only permitting) eddies in ocean reanalyses is important to infer the time-mean transports across 34.5°S, but it has minimal impact on the amplitude and variation of the monthly-mean transports in the reanalyses.

The 12-month running mean overturning and MHT over the whole ensemble period is relatively stable (Fig 3e,f), with similar ensemble-mean values over the whole period to those during the observational period (Table 2). The ensemble-mean MOC has no significant trend over 1993-2020. However, there is a significant increase in GloRan (1.18 Sv/decade) and ORAP6 (0.41 Sv/decade), and a significant decrease in CGLORS (-0.32 Sv/decade) and GLORYS (-0.60 Sv/decade). In contrast, only GloRan has a significant (increasing) trend in MHT (~0.042 PW/decade). GLORYS12v1 has no significant trend in MOC or MHT. Hence, there is uncertainty in the long-term trends from reanalyses.

The altimeter-based estimate has significant ($p < 0.05$) increases in MOC (~0.66 Sv/decade) and MHT (~0.036 PW/decade) over 1993-2020 and there is a significant increase in MHT over 1993-2016 in both the ORAS5- (~0.086 PW/decade) and ORAP6- (~0.094 PW/decade) based Mayer estimates. The Trenberth estimate has a significant but weak decline (~-0.010 PW/decade) over 2000-2016; the Mayer estimates also decline over this period, but the trend is insignificant. In the 12-month running mean estimates, the ensemble-mean is only weakly correlated with the altimeter-based estimate (r=0.24 for MOC and r = 0.25 for MHT), so their high monthly-mean correlation is largely due to similar seasonal variability.

The 12-month running mean from SAMBA is entirely different to other estimates (Fig 3e,f), with a rapid increase in the MOC (~14 Sv) and MHT (~0.7 PW) from March 2014 to June 2016, followed by a rapid decline. Although an extended SAMBA timeseries is needed to determine longer timescale variations, the large inter-annual variability over the observational period does not occur in other estimates. However, the Mayer MHT estimates have inter-annual variations of comparable (but smaller) magnitude before the SAMBA observational period (Fig 3f).

There is a clear annual cycle in the ensemble-mean and altimeter-based transports, unlike SAMBA (Fig 3c,d). While we show the ensemble-mean and altimeter-based seasonal cycles over the SAMBA observational period (Fig 4), the seasonal cycles derived over the full record lengths are similar (not shown). The ensemble and altimeter-based overturning are weakest in austral summer, but the ensemble is strongest in May/June, peaking two months after the altimeter-based estimate (Fig 4, upper panels). In contrast, the MOC in SAMBA is dominated

https://doi.org/10.5194/sp-2022-8
Preprint. Discussion started: 30 September 2022

by a semi-annual signal, with minima in April and September, and maxima in August and December. There are year-to-year variations in the seasonal cycles of all estimates (not shown), with variations in phase, shape and magnitude, but seasonal evolutions are far more variable in SAMBA than in the other estimates. In SAMBA, four years of observations are likely not long enough to obtain a robust seasonal cycle given the strong high-frequency variations.

The seasonal cycle in MHT is similar to that of the overturning for each estimate. The Mayer energy-budget estimates have seasonal cycles over the SAMBA period dominated by an annual signal, with a larger magnitude range than other estimates. They are similar to the Trenberth estimate, but with greater month-to-month variability. However, when they are averaged over the 2000-2016 period used in the Trenberth estimate, they become smoother and closer to the ensemble ("Mayer_ORAS5_2000-16" in Fig 4).

Inter-annual variations in the seasonal cycle of each estimate (not shown), and differences in the seasonal cycle between each estimate, stem from their geostrophic differences (Fig 4, lower panels), because the Ekman seasonal cycles are similar year-to-year (not shown) and for all estimates (Fig 4, middle panels). Differences between estimates are clearer in the geostrophic component, peaking before the ensemble-mean in the altimeter-based estimate and after the ensemble-mean in SAMBA. Thus, the Ekman and geostrophic components tend to oppose each other in the altimeter-based estimate and augment each other in SAMBA. This causes a greater increase in the magnitude of the total MOC and MHT seasonal cycles (relative to their geostrophic components) in SAMBA than it does in the altimeter-based estimate, but a greater change in the seasonal cycle phase and shape in the altimeter-based estimate (cf. Fig 4, lower and upper panels). The relative contribution of the Ekman component to the total MOC and MHT in the ensemble is nonetheless significantly greater than in SAMBA. In the ensemble-mean (and in the 1/12 degree GLORYS12V1 reanalysis and SAMBA), the geostrophic component of the MOC (Fig 4, lower left panel) has a second peak in November or December (i.e., austral spring or summer), and thus has a semi-annual signal. Although the increase in the MOC to this end-of-year peak relative to the magnitude of decrease from the preceding peak is smaller in the ensemble-mean than in SAMBA, it is noteworthy, increasing by 52% of the preceding decrease (and by 77% in the seasonal cycle over 1993-2020) compared to 84% in SAMBA. Over the SAMBA period, a significant increase in austral spring only occurs in the ensemble in 2014 and 2016, common to all reanalyses (not shown). The altimeter-based estimate has no significant increase in the geostrophic component in austral spring, and there is also no increase in the ensemble-mean MHT, unlike in SAMBA (Fig 4, lower right panel).

4 Conclusions

An ensemble of global ocean reanalyses from CMEMS provides a useful estimate of the magnitude and variability of the South Atlantic meridional overturning circulation and meridional heat transport, although it differs substantially from estimates based on SAMBA array data at 34.5°S, observed between 2013 and 2017. The ensemble is also compared with several other estimates of the overturning and heat transport, which also differ in many aspects from both the reanalyses and the SAMBA observations.

https://doi.org/10.5194/sp-2022-8
Preprint. Discussion started: 30 September 2022

The ensemble-mean (and 1/12 degree GLORYS12V1 reanalysis) transports have no long-term trend over 1993-2020, although the trends in the individual reanalyses differ, and observational estimates increase over this period. All estimates of the time-mean overturning are similar (~15.5 – 18.7 Sv), but there is relatively greater spread in the heat transport (0.35 – 0.61 PW), with the reanalyses ensemble weaker than SAMBA observations. Monthly-mean overturning and MHT in the ensemble, the 1/12 degree GLORYS12V1 reanalysis, and an altimeter-based estimate (Dong et al., 2021) vary significantly less than those from the SAMBA array. In contrast, energy-budget estimates of MHT (Mayer et al., 2022) have a large monthly-mean variability comparable to SAMBA. Both the monthly-mean overturning and MHT in the ensemble are significantly correlated with the altimeter-based estimate across the whole 1993-2020 period (although most of the skill is from the seasonal cycle), whereas correlations with SAMBA estimates are insignificant.

While there is inter-annual variability in the reanalyses and altimeter-based estimate over 1993-2020, SAMBA observations and some energy-budget MHT estimates have much larger inter-annual variability. The climatological seasonal cycles of the MOC and MHT vary considerably in phase and magnitude between estimates due to differences in the geostrophic flow, with good agreement in the Ekman contributions among all of the datasets considered. There is significant variation in their year-to-year cycles, most evident in SAMBA observations. A more in-depth analysis of each dataset is required to understand the causes of similarities and differences between the estimates, and hence to improve estimations. Differences between the observed estimates could be a result of differences in the spatial and temporal resolution of the datasets or the methods used to calculate them, but this remains an open question which needs further investigation. Exploring how well water masses are represented in the reanalyses, and analysing the density profiles and the spatial distribution of transports in each dataset would also be useful to understand the differences between the reanalyses and the observations. Reanalyses could inform whether improvements in observational density across the SAMBA array may provide more robust observational transport estimates.

To summarise, an ensemble of ocean reanalyses appears to be a useful tool to understand changes in the South Atlantic overturning and heat transport, and differences between estimates. They also enable variations prior to SAMBA to be estimated. Reanalyses and observations can be used together to improve our understanding of the overturning circulation and heat transport in the South Atlantic.

Data Availability

All data products used in this paper are listed in Table 1, along with their corresponding documentation and online availability.

Competing Interests

The authors declare that they have no conflict of interest.

https://doi.org/10.5194/sp-2022-8
Preprint. Discussion started: 30 September 2022

References

Baker, J. A., Watson, A. J., & Vallis, G. K. (2020). Meridional overturning circulation in a multibasin model. Part i: Dependence on southern ocean buoyancy forcing. *Journal of Physical Oceanography*, *50*(5), 1159–1178. https://doi.org/10.1175/JPO-D-19-0135.1

Baker, J. A., Watson, A. J., & Vallis, G. K. (2021). Meridional Overturning Circulation in a Multibasin Model. Part II: Sensitivity to Diffusivity and Wind in Warm and Cool Climates. *Journal of Physical Oceanography*, *51*(6), 1813–1828. https://doi.org/10.1175/JPO-D-20-0121.1

Biastoch, A., Schwarzkopf, F. U., Getzlaff, K., Rühs, S., Martin, T., Scheinert, M., Schulzki, T., Handmann, P., Hummels, R., & Böning, C. W. (1177). Regional imprints of changes in the Atlantic Meridional Overturning Circulation in the eddy-rich ocean model VIKING20X. *Ocean Sci*, *17*. https://doi.org/10.5194/os-17-1177-2021

Buckley, M. W., & Marshall, J. (2016). Observations, inferences, and mechanisms of the Atlantic Meridional Overturning Circulation: A review. *Reviews of Geophysics*, *54*(1), 5–63. https://doi.org/10.1002/2015RG000493

Caesar, L., Rahmstorf, S., Robinson, A., Feulner, G., & Saba, V. (2018). Observed fingerprint of a weakening Atlantic Ocean overturning circulation. *Nature 2018 556:7700*, *556*(7700), 191–196. https://doi.org/10.1038/s41586-018-0006-5

Dee, D. P., Uppala, S. M., Simmons, A. J., Berrisford, P., Poli, P., Kobayashi, S., Andrae, U., Balmaseda, M. A., Balsamo, G., Bauer, P., Bechtold, P., Beljaars, A. C. M., van de Berg, L., Bidlot, J., Bormann, N., Delsol, C., Dragani, R., Fuentes, M., Geer, A. J., … Vitart, F. (2011). The ERA-Interim reanalysis: configuration and performance of the data assimilation system. *Quarterly Journal of the Royal Meteorological Society*, *137*(656), 553–597. https://doi.org/10.1002/qj.828

Dong, S., Garzoli, S., Baringer, M., Meinen, C., & Goni, G. (2009). Interannual variations in the Atlantic meridional overturning circulation and its relationship with the net northward heat transport in the South Atlantic. *Geophysical Research Letters*, *36*(20). https://doi.org/10.1029/2009GL039356

Dong, S., Goni, G., & Bringas, F. (2015). Temporal variability of the South Atlantic Meridional Overturning Circulation between 20°S and 35°S. *Geophysical Research Letters*, *42*(18), 7655–7662. https://doi.org/10.1002/2015GL065603

Dong, S., Goni, G., Domingues, R., Bringas, F., Goes, M., Christophersen, J., & Baringer, M. (2021). Synergy of In Situ and Satellite Ocean Observations in Determining Meridional Heat Transport in the Atlantic Ocean. *Journal of Geophysical Research: Oceans*, *126*(4), e2020JC017073. https://doi.org/10.1029/2020JC017073

Frajka-Williams, E., Ansorge, I. J., Baehr, J., Bryden, H. L., Chidichimo, M. P., Cunningham, S. A., Danabasoglu, G., Dong, S., Donohue, K. A., Elipot, S., Heimbach, P., Holliday, N. P., Hummels, R., Jackson, L. C., Karstensen, J., Lankhorst, M., le Bras, I. A., Susan Lozier, M., McDonagh, E. L., … Wilson, C. (2019). Atlantic meridional overturning circulation: Observed transport and variability. *Frontiers in Marine Science*, *6*(JUN), 260. https://doi.org/10.3389/FMARS.2019.00260/BIBTEX

Garzoli, S. L., Baringer, M. O., Dong, S., Perez, R. C., & Yao, Q. (2013). South Atlantic meridional fluxes. *Deep Sea Research Part I: Oceanographic Research Papers*, *71*, 21–32. https://doi.org/10.1016/J.DSR.2012.09.003

Garzoli, S. L., & Matano, R. (2011). The South Atlantic and the Atlantic Meridional Overturning Circulation. *Deep Sea Research Part II: Topical Studies in Oceanography*, *58*(17–18), 1837–1847. https://doi.org/10.1016/J.DSR2.2010.10.063

Goes, M., Goni, G., & Dong, S. (2015). An optimal XBT-based monitoring system for the South Atlantic meridional overturning circulation at 34°S. *Journal of Geophysical Research: Oceans*, *120*(1), 161–181. https://doi.org/10.1002/2014JC010202

https://doi.org/10.5194/sp-2022-8
Preprint. Discussion started: 30 September 2022

Hawkins, E., Smith, R. S., Allison, L. C., Gregory, J. M., Woollings, T. J., Pohlmann, H., & de Cuevas, B. (2011). Bistability of the Atlantic overturning circulation in a global climate model and links to ocean freshwater transport. *Geophysical Research Letters*, *38*(10). https://doi.org/10.1029/2011GL047208

Hersbach, H., Bell, B., Berrisford, P., Hirahara, S., Horányi, A., Muñoz-Sabater, J., Nicolas, J., Peubey, C., Radu, R., Schepers, D., Simmons, A., Soci, C., Abdalla, S., Abellan, X., Balsamo, G., Bechtold, P., Biavati, G., Bidlot, J., Bonavita, M., … Thépaut, J. N. (2020). The ERA5 global reanalysis. *Quarterly Journal of the Royal Meteorological Society*, *146*(730), 1999–2049. https://doi.org/10.1002/QJ.3803

Jackson, L. C., Dubois, C., Forget, G., Haines, K., Harrison, M., Iovino, D., Köhl, A., Mignac, D., Masina, S., Peterson, K. A., Piecuch, C. G., Roberts, C. D., Robson, J., Storto, A., Toyoda, T., Valdivieso, M., Wilson, C., Wang, Y., & Zuo, H. (2019). The Mean State and Variability of the North Atlantic Circulation: A Perspective From Ocean Reanalyses. *Journal of Geophysical Research: Oceans*, *124*(12), 9141–9170. https://doi.org/10.1029/2019JC015210

Kersalé, M., Meinen, C. S., Perez, R. C., le Hénaff, M., Valla, D., Lamont, T., Sato, O. T., Dong, S., Terre, T., van Caspel, M., Chidichimo, M. P., van den Berg, M., Speich, S., Piola, A. R., Campos, E. J. D., Ansorge, I., Volkov, D. L., Lumpkin, R., & Garzoli, S. L. (2020). Highly variable upper and abyssal overturning cells in the South Atlantic. *Science Advances*, *6*(32). https://doi.org/10.1126/SCIADV.ABA7573/SUPPL_FILE/ABA7573_SM.PDF

Kersalé, M., Meinen, C. S., Perez, R. C., Piola, A. R., Speich, S., Campos, E. J. D., Garzoli, S. L., Ansorge, I., Volkov, D. L., le Hénaff, M., Dong, S., Lamont, T., Sato, O. T., & van den Berg, M. (2021). Multi-Year Estimates of Daily Heat Transport by the Atlantic Meridional Overturning Circulation at 34.5°S. *Journal of Geophysical Research: Oceans*, *126*(5), e2020JC016947. https://doi.org/10.1029/2020JC016947

Lellouche, J. M., le Galloudec, O., Drévillon, M., Régnier, C., Greiner, E., Garric, G., Ferry, N., Desportes, C., Testut, C. E., Bricaud, C., Bourdallé-Badie, R., Tranchant, B., Benkiran, M., Drillet, Y., Daudin, A., & de Nicola, C. (2013). Evaluation of global monitoring and forecasting systems at Mercator Océan. *Ocean Science*, *9*(1), 57–81. https://doi.org/10.5194/os-9-57-2013

Liu, C., Allan, R. P., Mayer, M., Hyder, P., Desbruyères, D., Cheng, L., Xu, J., Xu, F., & Zhang, Y. (2020). Variability in the global energy budget and transports 1985–2017. *Climate Dynamics*, *55*(11–12), 3381–3396. https://doi.org/10.1007/S00382-020-05451-8/FIGURES/5

Loeb, N. G., Doelling, D. R., Wang, H., Su, W., Nguyen, C., Corbett, J. G., Liang, L., Mitrescu, C., Rose, F. G., & Kato, S. (2018). Clouds and the Earth's Radiant Energy System (CERES) Energy Balanced and Filled (EBAF) Top-of-Atmosphere (TOA) Edition-4.0 Data Product. *Journal of Climate*, *31*(2), 895–918. https://doi.org/10.1175/JCLI-D-17-0208.1

MacLachlan, C., Arribas, A., Peterson, K. A., Maidens, A., Fereday, D., Scaife, A. A., Gordon, M., Vellinga, M., Williams, A., Comer, R. E., Camp, J., Xavier, P., & Madec, G. (2015). Global Seasonal forecast system version 5 (GloSea5): a high-resolution seasonal forecast system. *Quarterly Journal of the Royal Meteorological Society*, *141*(689), 1072–1084. https://doi.org/10.1002/qj.2396

Majumder, S., Schmid, C., & Halliwell, G. (n.d.). *An observations and model-based analysis of meridional transports in the South Atlantic*. https://doi.org/10.1002/2016JC011693

Mayer, J., Mayer, M., & Haimberger, L. (2021). Consistency and Homogeneity of Atmospheric Energy, Moisture, and Mass Budgets in ERA5. *Journal of Climate*, *34*(10), 3955–3974. https://doi.org/10.1175/JCLI-D-20-0676.1

Mayer, J., Mayer, M., Haimberger, L., & Liu, C. (2022). Comparison of Surface Energy Fluxes from Global to Local Scale. *Journal of Climate*, *1*(aop), 1–55. https://doi.org/10.1175/JCLI-D-21-0598.1

Meinen, C. S., Speich, S., Perez, R. C., Dong, S., Piola, A. R., Garzoli, S. L., Baringer, M. O., Gladyshev, S., & Campos, E. J. D. (2013). Temporal variability of the meridional overturning circulation at 34.5°S: Results from two pilot boundary arrays in the South Atlantic. *Journal of Geophysical Research: Oceans*, *118*(12), 6461–6478. https://doi.org/10.1002/2013JC009228

https://doi.org/10.5194/sp-2022-8
Preprint. Discussion started: 30 September 2022

Meinen, C. S., Speich, S., Piola, A. R., Ansorge, I., Campos, E., Kersalé, M., Terre, T., Chidichimo, M. P., Lamont, T., Sato, O. T., Perez, R. C., Valla, D., van den Berg, M., le Hénaff, M., Dong, S., & Garzoli, S. L. (2018). Meridional Overturning Circulation Transport Variability at 34.5°S During 2009–2017: Baroclinic and Barotropic Flows and the Dueling Influence of the Boundaries. *Geophysical Research Letters*, *45*(9), 4180–4188. https://doi.org/10.1029/2018GL077408

Mignac, D., Ferreira, D., & Haines, K. (2018). South Atlantic meridional transports from NEMO-based simulations and reanalyses. *Ocean Science*, *14*(1), 53–68. https://doi.org/10.5194/OS-14-53-2018

Nadeau, L. P., & Jansen, M. F. (2020). Overturning Circulation Pathways in a Two-Basin Ocean Model. *Journal of Physical Oceanography*, *50*(8), 2105–2122. https://doi.org/10.1175/JPO-D-20-0034.1

Perez, R. C., Garzoli, S. L., Meinen, C. S., & Matano, R. P. (2011). Geostrophic Velocity Measurement Techniques for the Meridional Overturning Circulation and Meridional Heat Transport in the South Atlantic. *Journal of Atmospheric and Oceanic Technology*, *28*(11), 1504–1521. https://doi.org/10.1175/JTECH-D-11-00058.1

Rahmstorf, S. (2015). Exceptional twentieth-century slowdown in Atlantic Ocean overturning circulation. *Nat. Clim. Chang.*, *5*(5), 475–480. https://doi.org/10.1038/nclimate2554

Storto, A., Masina, S., & Navarra, A. (2016). Evaluation of the CMCC eddy-permitting global ocean physical reanalysis system (C-GLORS, 1982-2012) and its assimilation components. *Quarterly Journal of the Royal Meteorological Society*, *142*(695), 738–758. https://doi.org/10.1002/qj.2673

Thornalley, D. J. R., Oppo, D. W., Ortega, P., Robson, J. I., Brierley, C. M., Davis, R., Hall, I. R., Moffa-Sanchez, P., Rose, N. L., Spooner, P. T., Yashayaev, I., & Keigwin, L. D. (2018). Anomalously weak Labrador Sea convection and Atlantic overturning during the past 150 years. *Nature 2018 556:7700*, *556*(7700), 227–230. https://doi.org/10.1038/s41586-018-0007-4

Trenberth, K. E., Zhang, Y., Fasullo, J. T., & Cheng, L. (2019). Observation-Based Estimates of Global and Basin Ocean Meridional Heat Transport Time Series. *Journal of Climate*, *32*(14), 4567–4583. https://doi.org/10.1175/JCLI-D-18-0872.1

Weijer, W., Cheng, W., Drijfhout, S. S., Fedorov, A. v., Hu, A., Jackson, L. C., Liu, W., McDonagh, E. L., Mecking, J. v., & Zhang, J. (2019). Stability of the Atlantic Meridional Overturning Circulation: A Review and Synthesis. *Journal of Geophysical Research: Oceans*, *124*(8), 5336–5375. https://doi.org/10.1029/2019JC015083

Weijer, W., Cheng, W., Garuba, O. A., Hu, A., & Nadiga, B. T. (2020). CMIP6 Models Predict Significant 21st Century Decline of the Atlantic Meridional Overturning Circulation. *Geophysical Research Letters*, *47*(12), e2019GL086075. https://doi.org/10.1029/2019GL086075

Weijer, W., de Ruijter, W. P. M., Sterl, A., & Drijfhout, S. S. (n.d.). *Response of the Atlantic overturning circulation to South Atlantic sources of buoyancy*. Retrieved April 12, 2022, from www.elsevier.com/locate/gloplacha

Xu, X., Chassignet, E. P., Dong, S., & Baringer, M. O. (2022). Transport Structure of the South Atlantic Ocean Derived From a High-Resolution Numerical Model and Observations. *Frontiers in Marine Science*, *0*, 175. https://doi.org/10.3389/FMARS.2022.811398

Zuo, H., Balmaseda, M. A., Tietsche, S., Mogensen, K., & Mayer, M. (2019). The ECMWF operational ensemble reanalysis-analysis system for ocean and sea ice: A description of the system and assessment. *Ocean Science*, *15*(3), 779–808. https://doi.org/10.5194/os-15-779-2019

Zuo, H., Balmaseda, M. A., de Boisseson, E., Tietsche, S., Mayer, M., and de Rosnay, P. (2021). The ORAP6 ocean and sea-ice reanalysis: description and evaluation. EGU General Assembly 2021, online, 19–30 Apr 2021, EGU21-9997, https://doi.org/10.5194/egusphere-egu21-9997, 2021.

https://doi.org/10.5194/sp-2022-8
Preprint. Discussion started: 30 September 2022

Ref. No.	Product name & type	Documentation
1	GLOBAL_REANALYSIS_PHY_001_031, Reanalysis (C-GLORSv7 and GLORYS2V4 ocean reanalyses) [1993-2020]	QUID: http://marine.copernicus.eu/documents/QUID/CMEMS-GLO-QUID-001-031.pdf PUM: http://marine.copernicus.eu/documents/PUM/CMEMS-GLO-PUM-001-031.pdf
2	ORAP6 global ocean reanalysis [1993-2020]	Updated version of the ORAS5 reanalysis from GLOBAL_REANALYSIS_PHY_001_031 listed in Product Ref 1 The updated CMEMS global ocean reanalysis ensemble containing this reanalysis will be available online soon. See Zuo et al (2021): https://doi.org/10.5194/egusphere-egu21-9997
3	GloRanV14 global ocean reanalysis [1993-2021]	Updated version of the FOAM/GLOSEA5 reanalysis from GLOBAL_REANALYSIS_PHY_001_031 listed in Product Ref 1 The updated CMEMS global ocean reanalysis ensemble containing this reanalysis will be available online soon.
4	GLOBAL_MULTIYEAR_PHY_001_030 (GLORYS12V1 ocean reanalysis) [1993-2019]	QUID: https://catalogue.marine.copernicus.eu/documents/QUID/CMEMS-GLO-QUID-001-030.pdf PUM: https://catalogue.marine.copernicus.eu/documents/PUM/CMEMS-GLO-PUM-001-030.pdf
5	South Atlantic Meridional Overturning Circulation – Basin-wide Array (SAMBA) observations for 2013-2017 (Kersalé et al. 2020 (for MOC), Kersalé et al. 2021 (for MHT)	https://www.aoml.noaa.gov/phod/research/moc/samoc/sam/data_access.php https://www.aoml.noaa.gov/phod/SAMOC_international/samoc_data.php
6	Blended in situ and satellite altimeter estimates for 1993-2021 (Dong et al., 2021)	See Dong et al (2021): https://doi.org/10.1029/2020JC017073
7	Energy-budget estimates of Mayer et al., 2022 [1993-2017]	Atmospheric energy budgets using ERA5 available at https://cds.climate.copernicus.eu/cdsapp#!/dataset/derived-reanalysis-energy-moisture-budget?tab=overview TOA radiation data from University of Reading: https://researchdata.reading.ac.uk/271/
8	Energy-budget estimates of Trenberth et al., 2019 [2000-2016]	https://gdex.ucar.edu/dataset/Ocean_MHT_Values.html

Table 1: Data products used in this study, including documentation where available.

435

https://doi.org/10.5194/sp-2022-8
Preprint. Discussion started: 30 September 2022

Variable	Statistic	Ocean reanalyses		SAMOC Estimates		Energy-budget estimates		
		Ensemble	GLORYS12V1	SAMBA	Altimeter Dong	Trenberth	Mayer ORAS5	Mayer ORAP6
MOC (Sv)	Mean ± uncertainty (2013-17)	16.56 ± 0.37	18.72	17.29 ± 5.0	18.69	-	-	-
	Monthly-mean variability	2.67	2.90	11.35	3.25	-	-	-
	Mean ± uncertainty (1993-2020)	16.38 ± 0.66	19.23	-	18.34	-	-	-
	Monthly-mean variability	3.00	3.30	-	3.48	-	-	-
	Trends (Sv/decade) (1993-2020)	0.17 (NS)	-0.08 (NS)	-	0.66	-	-	-
MHT (PW)	Mean ± uncertainty (2013-17)	0.36 ± 0.03	0.44	0.50 ± 0.23	0.61	-	0.31	0.31
	Monthly-mean variability	0.19	0.20	0.55	0.20	-	0.46	0.43
	Mean ± uncertainty (1993-2020)	0.37 ± 0.04	0.49	-	0.58	0.33 (2000-16)	0.33 (1993-2017)	0.34 (1993-2017)
	Monthly-mean variability	0.20	0.23	-	0.21	-	0.40	0.44
	Trends (PW/decade) (1993-2020)	-0.001 (NS)	-0.007 (NS)	-	0.036	-0.010 (2000-16)	0.086 (1993-2016)	0.094 (1993-2016)

Table 2: Time-mean and uncertainty (or ensemble spread), monthly-mean variability and trends of the maximum MOC and the MHT across 34.5°S, for the ensemble-mean (product ref's 1, 2, 3), GLORYS12V1 (product ref 4), SAMBA observations (product ref. 5), an altimeter-based estimate (product ref 6) and energy-budget estimates (product ref's 7 and 8). All volume transports are referenced to zero at the surface. Time-mean values are calculated over the 2013-2017 SAMBA observational period and over the full 1993-2020 ensemble period, if available. Uncertainty in the ensemble-mean is defined as the standard error of the time-mean transport across the ensemble (note: this is smaller than the true uncertainty in the estimate). Monthly-mean variability (i.e., a measure of the deviation of monthly-mean data from the time-mean) is defined as the standard deviation of the monthly-mean transports over the timeseries. Methods used to calculate SAMBA observational uncertainty (Kersalé et al., 2020, 2021) are described in Meinen et al., 2013 and Kersalé et al., 2021. Trends that are statistically insignificant are labelled NS.

https://doi.org/10.5194/sp-2022-8
Preprint. Discussion started: 30 September 2022

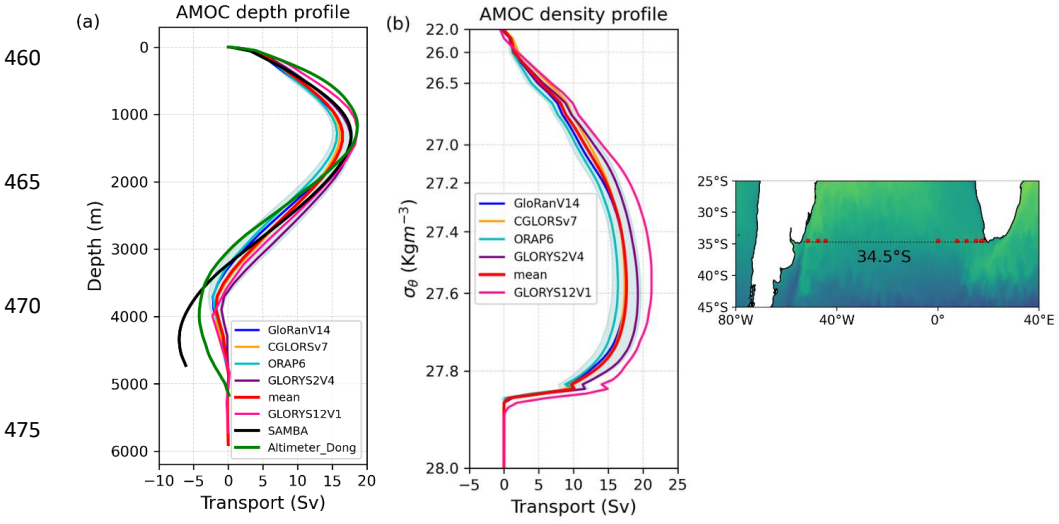

Figure 1: Vertical profile of the overturning transport across 34.5°S in (a) depth space and (b) density space, averaged over the 2013-2017 period of SAMBA observations, from September 2013 to July 2017. The reanalyses ensemble-mean (red, product ref's 1, 2, 3) and spread (light cyan shading) are plotted, along with each ensemble member, the GLORYS12V1 reanalysis (pink, product ref 4), the SAMBA observations (black, product ref. 5) and an altimeter-based estimate (green, product ref 6). The ensemble spread is defined as two times the standard deviation across the ensemble members. (right panel) Map showing the location of the SAMBA moorings (red dots) along 34.5°S.

https://doi.org/10.5194/sp-2022-8
Preprint. Discussion started: 30 September 2022

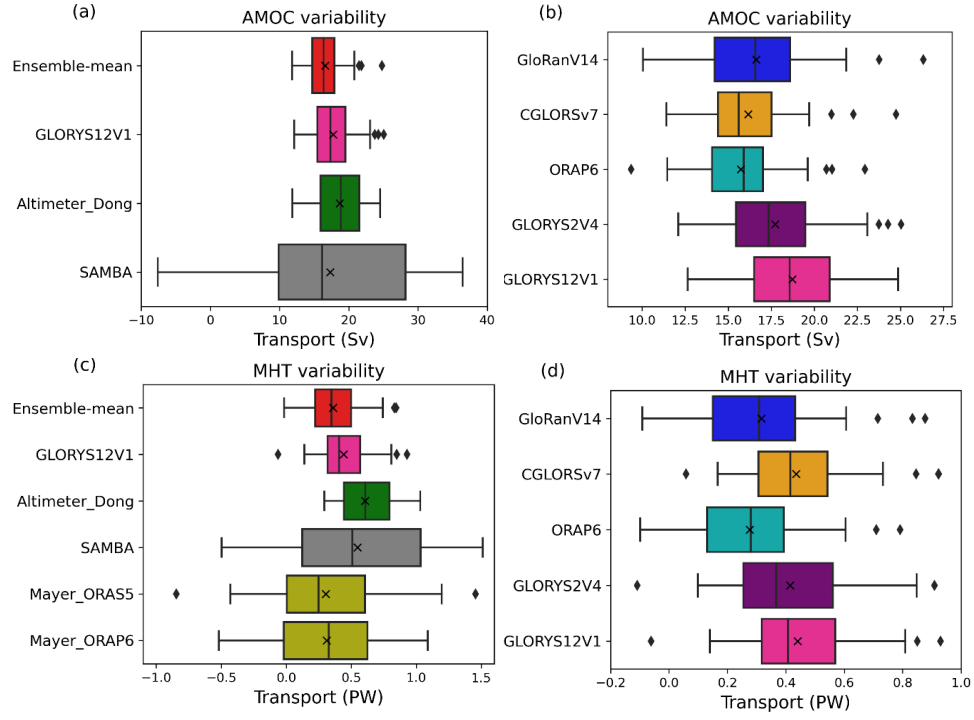

Figure 2: Whisker-box plots of the monthly-mean MOC (top panels) and MHT (bottom panels) across 34.5°S, over the SAMBA observational period (2013-2017), using the same products as in Fig 1. Energy-budget estimates, "Mayer_ORAP6" and "Mayer_ORAS5", (yellow, product ref 7) are also used for the MHT. Reanalyses analysed are shown in (b) and (d) with a reduced scale to highlight the differences between models. Boxes represent the interquartile range (IQR) with the median (line) and mean (crosses) shown. Whiskers cover a range of values up to one IQR beyond the upper and lower quartiles, and diamonds are outlying values beyond this range. Note: the x-axis scale changes between the left- and right-hand plots.

https://doi.org/10.5194/sp-2022-8
Preprint. Discussion started: 30 September 2022

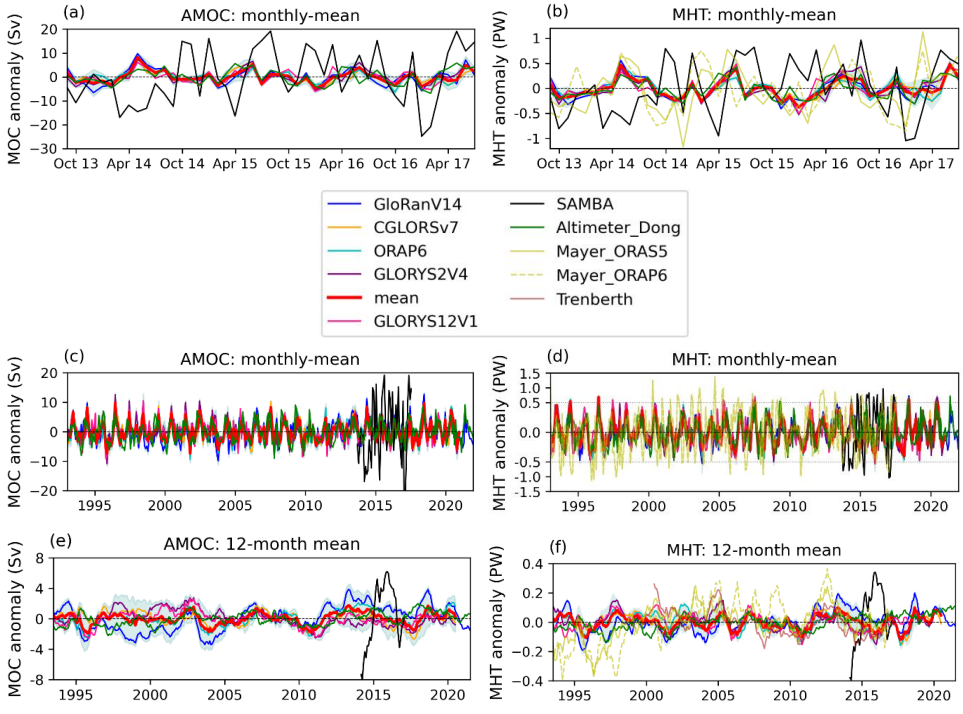

Figure 3: Timeseries of the monthly overturning (left) and heat transport (right) anomalies nominally across 34.5°S, with monthly-mean values from September 2013 to July 2017 (top panels) and over 1993-2021 (middle panels), and 12-month running mean values over 1993-2021 (bottom panels), in the four reanalyses, ensemble-mean (red), GLORYS12V1 (pink), SAMBA observations (black), an altimeter-based estimate (green) and energy-budget estimates (yellow and brown, product ref 8). Labels and shading as in Fig 1. The horizontal grey dashed lines in (d) divide the y-axis into two linear scales, with the y-axis compressed above the line. Note: Trenberth energy-budget estimate is for latitude, 33.5°S.

https://doi.org/10.5194/sp-2022-8
Preprint. Discussion started: 30 September 2022

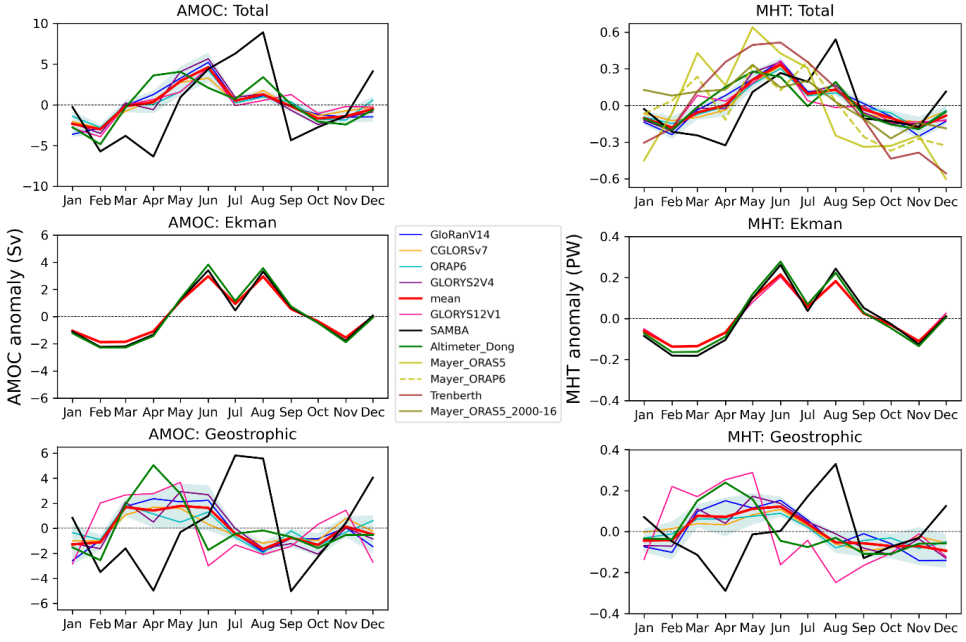

555 **Figure 4: Seasonal cycles of (left) the overturning and (right) the MHT anomalies across 34.5°S, averaged over the SAMBA observational period from September 2013 to July 2017. The exception is the energy-budget MHT estimate of Trenberth et al., 2019, which is averaged over 2000-2016, and also the ORAS5-based Mayer energy-budget estimate, "Mayer_ORAS5_2000-16" (olive), is averaged over the same period for comparison. The total (top panels), Ekman (middle panels) and geostrophic (bottom panels)**
560 **components of these transports are plotted. Labels, shading and product information are as in Figs 1 and 3.**